



HAL
open science

Ho:LuAG single crystal fiber: growth, spectroscopy and laser characteristics

Jian Liu, Qingsong Song, Zhanxin Wang, Yinyin Wang, Jifei Dong, Jie Xu, Peng Liu, Dongzhen Li, Jianlei Wang, Chun Wang, et al.

► To cite this version:

Jian Liu, Qingsong Song, Zhanxin Wang, Yinyin Wang, Jifei Dong, et al.. Ho:LuAG single crystal fiber: growth, spectroscopy and laser characteristics. *Optics Express*, 2022, 30 (4), pp.5826. 10.1364/OE.449790 . hal-03596864

HAL Id: hal-03596864

<https://hal.science/hal-03596864>



Submitted on 4 Mar 2022

HAL is a multi-disciplinary open access archive for the deposit and dissemination of scientific research documents, whether they are published or not. The documents may come from teaching and research institutions in France or abroad, or from public or private research centers.

L'archive ouverte pluridisciplinaire **HAL**, est destinée au dépôt et à la diffusion de documents scientifiques de niveau recherche, publiés ou non, émanant des établissements d'enseignement et de recherche français ou étrangers, des laboratoires publics ou privés.



Ho:LuAG single crystal fiber: growth, spectroscopy and laser characteristics

JIAN LIU,¹ QINGSONG SONG,¹ ZHANXIN WANG,² YINYIN WANG,²
JIFEI DONG,² JIE XU,² PENG LIU,² DONGZHEN LI,²  JIANLEI
WANG,³ CHUN WANG,³ KHEIRREDDINE LEBBOU,⁴ YANYAN XUE,¹
JUN XU,^{1,5} XIAODONG XU,^{2,6} AND YONGGUANG ZHAO^{2,7} 

¹School of Physics Science and Engineering, Institute for Advanced Study, Tongji University, Shanghai 200092, China

²Jiangsu Key Laboratory of Advanced Laser Materials and Devices, School of Physics and Electronic Engineering, Jiangsu Normal University, Xuzhou 221116, China

³Center for Optics Research and Engineering, Shandong University, Qingdao 266237, China

⁴Institut Lumière Matière, UMR5306 Université Lyon I - CNRS, Université de Lyon, Lyon 69622, Villeurbanne Cedex, France

⁵xujun@mail.shnc.ac.cn

⁶xdxu79@jsnu.edu.cn

⁷yongguangzhao@yeah.net

Abstract: Lutetium aluminum garnet single-crystal fiber (SCF, $\sim \Phi$ 0.9 mm – 165 mm) doped with 0.5 at.% Ho³⁺ has been grown by the micro-pulling-down (μ -PD) technique. The room-temperature absorption and emission spectra exhibit similar features to the bulk crystal. Laser performances of the SCFs with two different pump configurations, i.e., pump guiding and free-space propagation, are studied by employing a 1.9- μ m laser diode and a high-brightness fiber laser, respectively. Laser slope efficiencies obtained with both pump configurations can be higher than 50%, and a maximum output power of 6.01 W is achieved at \sim 2.09 μ m with the former pump. The comparable efficiency to the high-brightness pump is an indication of that high laser performance can also be expected through pump-guiding in the SCF even with a low pump beam quality.

© 2022 Optica Publishing Group under the terms of the [Optica Open Access Publishing Agreement](#)

1. Introduction

Solid-state lasers in the 2- μ m spectral range are of increasing interest [1] due to their widespread applications in eye-safe LIDAR [2–4], medical surgery [5], material processing [1,6] and as pump source to generate mid-IR lasers through optical parametric oscillators (OPOs) [7]. Compared to the Tm³⁺ ions, Ho³⁺-doped laser materials exhibit approximately five time larger cross section at a slightly longer emission wavelength from the transition of ⁵I₇ → ⁵I₈ where ⁵I₈ represents the ground state [8]. This enables direct in-band pumping of Ho-doped materials using 1.9- μ m sources such like Tm-fiber laser, yielding a relatively high laser quantum efficiency (>90% [9]) and high-power scalability [10]. Consequently, high-efficient laser operation at 2 μ m with straightforward thermal management can be achieved in combination with a fiber-like thin rod structure, i.e., the so called single crystal fiber (SCF) with a typical diameter of less than 1 mm and a length of few centimeters [11], offering a high surface-to-volume ratio like glass fiber while retaining the spectroscopic and thermomechanical properties of the bulk crystal. In addition, transverse laser mode is free-space propagation in the SCF, which in principle will have a good beam quality simply by inserting an aperture in the cavity to suppress the high-order transverse modes [12]. Common methods used for fabrication of SCFs are micro-pulling-down (μ -PD) [13], edge-defined film fed growth (EFG) [14], and laser heated pedestal growth (LHPG) [15]. In comparison, the μ -PD technique is promising for fabrication of large scale SCFs without

requirement of any additional polishing of the cylinder for pump guiding [16]. To date, 35.2 W of continuous-wave (CW) laser [12] and nanosecond pulse (7.5-ns) with a pulse energy of 1.44 μJ [17] have been reported from such Ho:YAG SCFs laser in-band pumped by a Tm-fiber laser at 1.9 μm. Moreover, laser operations of Ho-doped SCFs with other host materials like CNGG [18] and LiLuF₄ [19] have also been demonstrated, showing the high quality of the fabricated SCFs with such μ-PD method and the promising applications for lasing both in CW and pulse regimes.

Lutetium aluminum garnet, Lu₃Al₅O₁₂ (LuAG), similar to the well-known Y₃Al₅O₁₂ (YAG) crystal, belongs to the isostructural garnet family and exhibits high thermal conductivity as well as excellent physical and chemical properties [20,21]. The LuAG was reported as congruent material, so it is possible to grow undoped and RE³⁺-doped LuAG single crystals from the melt by the μ-PD technique [22–24]. From the other side, a slight difference of the lattice constant, i.e., 12.0075 and 11.9164 Å, respectively for YAG and LuAG [24], results in a stronger crystal field for the latter and thus enhances the Stark effect of the doped active ions like Ho³⁺. The large manifold splitting of the Ho³⁺ is favorable for branching ratios of ⁵I₇ → ⁵I₈ transition at room temperature [25] and beneficial for laser performance at 2.1 μm through slightly reducing the lower laser thermal population of Ho:LuAG [26]. However, laser performance of Ho:LuAG crystal in a SCF geometry, to the best of our knowledge, has never been investigated.

In this work, Ho³⁺-doped LuAG SCF has been grown by the micro-pulling-down technique, its room-temperature spectral properties including absorption and emission spectra are studied. The first laser operation based on Ho:LuAG SCF is thereafter experimentally demonstrated by using two different pump configurations, the corresponding intrinsic slope efficiency and propagation loss are also analyzed.

2. Crystal growth and optical spectroscopy

A Ho³⁺-doped LuAG SCF was grown by the μ-PD method under high-purity flowing nitrogen (N₂) atmosphere for iridium (Ir) crucible oxidation protection. The starting raw materials were crackle Ho:LuAG crystals grown by the Czochralski method. The Ho concentration was 0.5 at.% with respect to Lu³⁺. The crackle was melt in an Ir crucible, and a <111> oriented undoped LuAG crystal was used as a seed to contact to the crucible die for the SCF growth initiation. The upper image in Fig. 1 shows the schematic of the μ-PD method, the circular capillary die with an outer diameter of less than 1 mm locates at the middle of the conical bottom. The pulling rate was fixed at 0.5 mm/min over the entire growth period. Note that, a 0.5-mm-long liquid zone was existed below the crucible capillary die during the fabrication process, which means the SCF was pulled down with a meniscus outside the capillary die. Thus, to ensure a constant diameter of the SCF, control of the radio-frequency heating power was necessary through real-time monitoring of growing crystal from the observation window using a CCD camera. The lower image shows the as-grown Ho:LuAG SCF that has a length of 165 mm and a diameter of ~ 0.9 mm. The lateral surface of the SCF is inherently smooth due to the nature growth along <111> direction and thus no polishing is necessary for the total reflection of light during the laser operation.

A 2-mm-long segment that was directly cut from the as-grown 0.5 at.% Ho:LuAG SCF and thereafter optical polished on both ends, was used as a sample for the spectral characterization. Figure 2(a) shows its room-temperature absorption spectrum in a spectral range of 400 - 2000 nm, recorded by using a UV–VIS–NIR spectrophotometer (Model Cary-5000, Varian, USA). The absorption peaks located at 419 nm, 454 nm, 538 nm, 636 nm, and 1906 nm correspond to the transitions from ⁵I₈ ground state to ⁵G₅, ⁵G₆+⁵F₁, ⁵S₂+⁵F₄, ⁵F₅, and ⁵I₇ excited states. To perform the in-band pumping for the 2.1-μm laser operation, the highest absorption peak is located at 1906 nm with an absorption coefficient of 0.59 cm⁻¹. The strongest absorption peak matches well with the Ho:LuAG ceramic [27]. The absorption coefficient at 1907 nm is 0.46 μm⁻¹, giving theoretical single-pass absorptions (after considering the Fresnel loss) of 61% and 85%, for 20- and 40-mm-long SCFs, respectively.

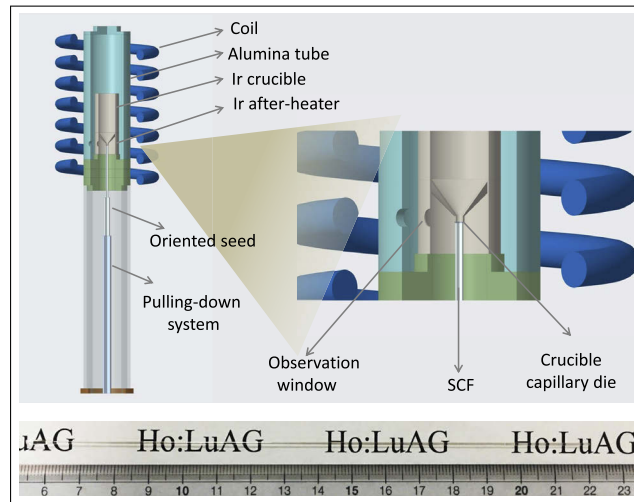


Fig. 1. Upper image shows the schematic illustration of the μ -PD method used for SCF growth, and the lower image shows the as-grown 165 mm long Ho:LuAG SCF.

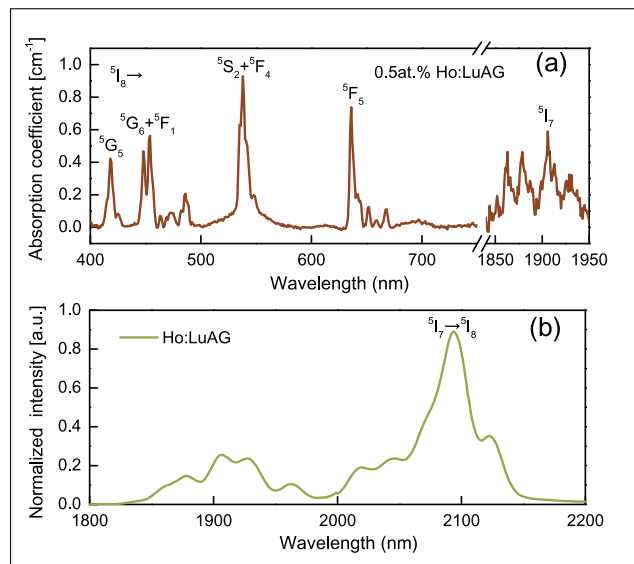


Fig. 2. Room-temperature absorption (a) and emission (b) spectra of 0.5 at.% Ho:LuAG SCF.

According to the absorption peaks of the Ho:LuAG SCF, a laser diode at 640 nm was used as the excitation source for the room-temperature emission spectra with a FLSP920 spectrometer. As shown in Figure 2(b), the profile of the fluorescence spectra is similar to the previous reported Ho:LuAG bulk crystals [28]. The emission spectrum from the transition of $^5I_7 \rightarrow ^5I_8$ of Ho^{3+} covers a broad wavelength range from 1800 to 2200 nm, with an emission peak located at 2097 nm. Note that, since the probably non-uniform distribution of active ions in the transvers cross section of the SCF [29], the emission cross sections of Ho:LuAG SCF are unable to be calculated for now.

3. CW laser operation

3.1. CW laser pumped by high-brightness Tm-fiber laser

Figure 3(a) shows the schematic of the CW Ho:LuAG SCF laser pumped with a homemade Tm-doped all-fiber laser (TDFL) delivering a maximum power of 30 W at 1907 nm [17]. The pump light was at first collimated by a lens (L1) with a focal length of $f_1 = 15$ mm, then passing through a 45 degree folding mirror, and finally focused onto the SCF by another lens (L2) with $f_2 = 100$ mm (Lens with focal lengths of 150 and 200 mm were also tested). Since the high beam quality of the Tm-fiber laser ($M^2 \sim 1.3$), the focused pump beam with a diameter of 166- μm had a depth of focus of around 18 mm. Thus, free space propagation rather than wave-guiding design for the pump light was employed to better match with the laser mode. A simple plane-plane cavity with both mirrors placed as close as possible to the SCF, was used to form the laser cavity. Because the calculated beam diameters on the both end facets were less than 350 μm , i.e., much smaller than the aperture of the SCF, the diffraction loss was ignored in our case. The pump mirror (PM) was coated for high transmission at 1850 – 1950 nm and high reflectivity at 2050 – 2250 nm. The transmissions of the output couplers (OCs) are 20%, 50%, and 83%. A dichroic mirror (DM) was used as a beam splitter for pump and laser beams. At last the laser was recorded by using a power meter Nova II equipped with 30(150)A-BB-18 probe. A Ho:LuAG SCF sample with 40 mm in length and 930 μm in diameter was employed as the laser gain medium. As can be seen the inset of Fig. 3, the transverse cross section of the SCF is not circular which in fact represents some nature facets of the LuAG garnet crystal. To avoid the feedback of the pump laser, both its end faces were optically polished and anti-reflection coated at both the pump and laser wavelength. To mitigate the thermal effect, the SCF was mounted in a special designed aluminum module and could be directly water-cooled to 10°C. Finally, a dichroic mirror, M3, was used to separate the residual pump and laser beams. The photograph of end facet of Ho:LuAG SCF with nearly 0.93 μm was also shown in Figure 3(b).

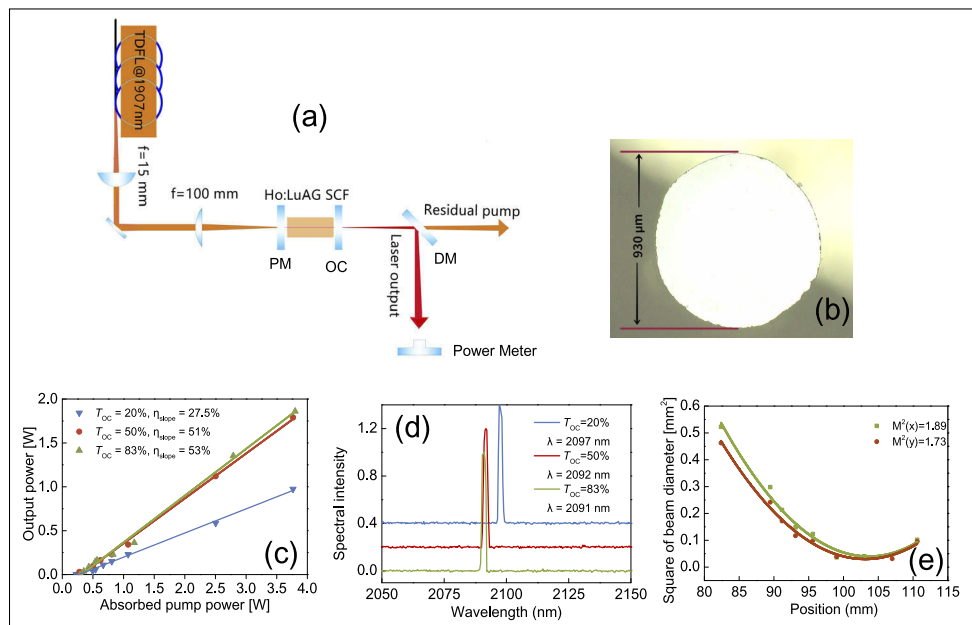


Fig. 3. Schematic of the Ho:LuAG SCF laser in-band pumped by a Tm-fiber laser at 1907 nm (a) and photograph of the end facet of the SCF (b); Output power (c) and optical spectra (d) of the Ho:LuAG SCF laser at different OCs; beam quality (e) of the Ho:LuAG SCF laser.

CW laser performance was studied with a physical cavity length of ~ 40 mm, almost same to the length of Ho:LuAG SCF by placing the cavity mirrors as close as to the SCF. At first, different pump beam waists, i.e., 83, 125, and 166 μm by using lenses with focal lengths of 100, 150 and 200 mm, were tested. Below the absorbed pump power of 4 W, the highest output power was achieved with the highest pump intensity (i.e., 83- μm beam radius). The reverse dependence of the laser power with the pump beam radius indicates that the pump intensity is even more critical than mode-matching at such a low pump level. Figure 3(c) shows the laser performance with respect to the absorbed pump power. As expected, the output laser was measured to be unpolarized. At an absorbed pump power of 3.8 W, the maximum output power of 1.86 W was achieved with $T_{OC} = 83\%$, corresponding to a slope efficiencies of 53%. The slope efficiency is almost the same as that of 53.3% from the Ho:YAG SCF laser with 92% OC [12]. In all the cases no power rollover phenomena were observed with the absorbed power, however, further power scaling was unavailable because of the serious feedback of the pump light from the OCs to the Tm-fiber laser. Nevertheless, the linear dependence with the pump power indicates the potential of Ho:LuAG SCF for laser operation at 2 μm . The work of this part is just a proof-of-principle study of the high-efficient laser operation based on such Ho:LuAG SCF fabricated using the μ -PD method. The higher laser output pumped by LD will also be introduced in detail in the next part.

Figure 3(d) shows the optical spectra of the Ho:LuAG SCF laser measured by using a high-resolution optical spectrum analyzer (OSA, AQ6375, YOKOGAWA). Single wavelength laser operation without satellites was found for the cases with different OCs. An obvious red-shift of the wavelength from 2091 to 2097.1 nm was observed with decreasing the transmissions of the OCs. This, as a typical phenomenon for the quasi-three-level laser system, could be attributed to the lower population inversion required for lasing in the case of a lower OC transmission, and thus leading to a stronger reabsorption effect [30].

The beam propagation factors (M^2) were measured using a CCD camera at an output power of 1 W with $T_{OC} = 83\%$. As shown in Figure 3(e), the values at x - and y -direction were calculated to be 1.89 and 1.73, respectively. The difference of M^2 factor between the two directions can be explained by the slight misalignment between the pump and oscillation axis in the horizontal plane, which will introduce more high-order transverse modes in the x -direction.

3.2. Laser operation with pump-guiding using a laser diode

The experimental setup of the laser-diode-pumped Ho:LuAG SCF laser is schematically shown in Fig. 4(a). In this case, a 20-mm-long Ho:LuAG SCF which was cut from the same as-grown SCF, was used as the laser gain medium with both end faces were polished and coated. The only reason we did not choose the 40-mm-long SCF was because of the physical damage at one end face of the SCF. The fiber-coupled (core diameter 400 μm , NA = 0.22, $M^2=54$) laser diode had a maximum output power of 28 W, the emission wavelength exhibited a red-shift from 1900 to 1906 nm as the power increased from 2.6 W to the highest. So, the wavelength at the higher laser power will better match the absorption peak of the Ho:LuAG SCF. From our recent work, it was found that mode matching is still a critical factor for high performance laser operation [31], so, mode-matching between the pump and the laser beams was considered in the following laser experiment. By using two plane-convex lens with focal lengths of 30 mm and 25 mm, the pump light was collimated and focused to a beam radius of ~ 180 μm at $z = 2$ mm along the Ho:LuAG SCF. To mitigate the thermal load, the sample was water-cooled to 10°C. The cavity comprised a plane input mirror and plane-concave output couplers (radius of curvature of 100 mm) with transmissions of 10%, 20%, and 50%. Since the large divergence of the pump light in the SCF, the spatial intensity distribution along the z -axis (propagation direction) was simulated by using ray-tracing analysis [32] and shown in in Fig. 4(b). As can be seen, the pump light was free-space propagation only in the front part and thereafter pump guiding in the 16-mm-long

rear part of the SCF. Moreover, obviously higher pump intensity was found in the central cross section, which will be beneficial for lasing in contrast to the traditional bulk materials.

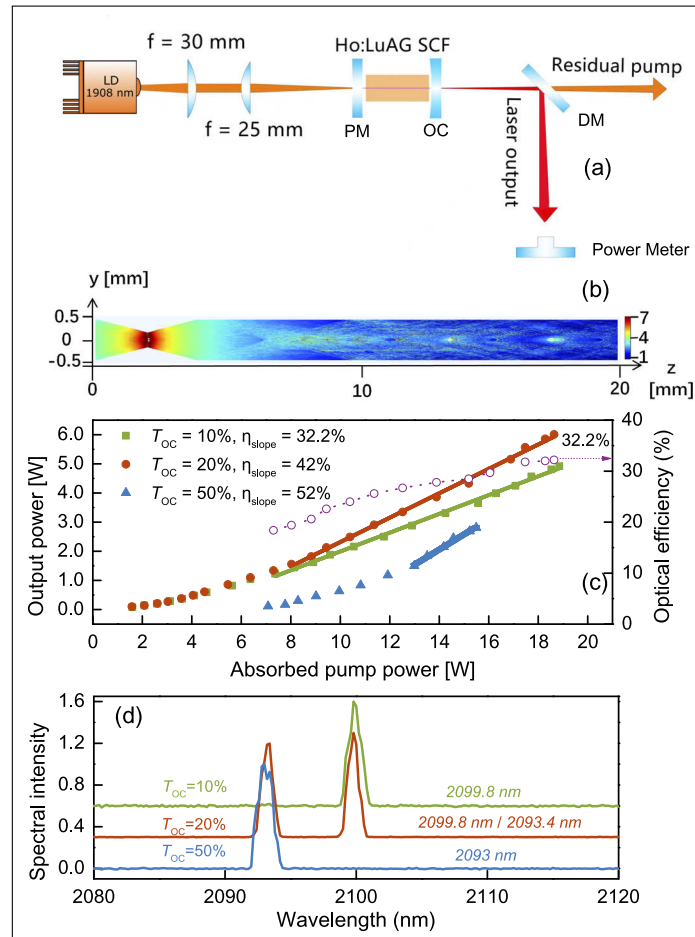


Fig. 4. Schematic of the Ho:LuAG SCF laser in-band pumped by a 1.9- μ m laser diode (a) and the simulated pump intensity distribution in the SCF by using ray-tracing analysis (b). Output power (c) and optical spectra (d) of the Ho:LuAG SCF laser for different OCs.

The output power of the Ho:LuAG SCF laser as a function of the absorbed pump power is shown in Fig. 4(c). For $T_{OC} = 20\%$, the single-pass absorption under lasing conditions was measured to be 61% for 2.58 W incident pump power, but increased to 68.5% in the case of 27.23 W. The increase was mainly due to the better wavelength match with the absorption peak of the Ho:LuAG SCF. A maximum continuous wave (CW) output power of 6.01 W with 42% slope efficiency was achieved at the highest pump power. It is worth mentioning that the maximum slope efficiency of 52% was achieved with $T_{OC} = 50\%$. This is comparable to the highest slope efficiency achieved with high-brightness pump configuration, which indicates that high laser performance can be realized through pump-guiding in the SCF even with a low pump beam quality. In all the cases, no power rollover was observed and further power scaling was limited just by the available pump power, which on the other hand indicates a good optical quality of the Ho:LuAG SCF grown by the μ -PD method. Laser output was not obtained for the OC with transmission of 83% in the diode pumped experiment. We notice that the output dependences are non-linear above the laser threshold. At Lower pump power, parts of the Ho:LuAG SCF

far from the pump light are not sufficiently excited, which is not conducive to efficient laser output. Figure 4(d) shows the optical spectra of Ho:LuAG SCF laser for different OCs, the peak wavelength shifted from 2099.8 nm to 2093 nm with the increase of the OCs.

The resonator losses and intrinsic slope efficiency were thereafter calculated by using the modified CaIRD analyses in the case of large OC transmission [33]:

$$\frac{1}{\eta_s} = \frac{1}{\eta_0} \left(1 + \frac{2\gamma}{-\ln(R_{OC})} \right), \quad (1)$$

$$\gamma = -\ln(1 - L). \quad (2)$$

where η_0 is the intrinsic slope efficiency, R_{OC} represents the reflectivity of the output mirrors, and L is the internal loss of per pass. As shown in Fig. 5(a), the resonator loss was calculated to be 0.021 cm^{-1} , less than half that of the Ho:YAG SCF [12]. And the intrinsic slope efficiency was 58.2%, which is comparable with that of Ho:YAG SCF (60%) [12], but still less than the quantum efficiency of $\sim 91\%$.

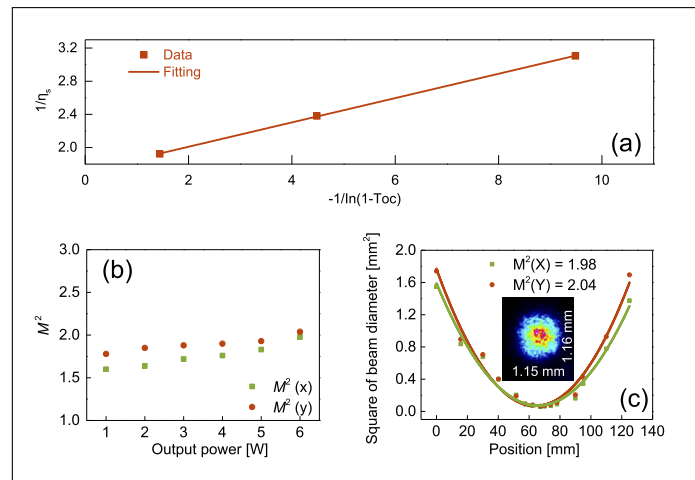


Fig. 5. CaIRD plot (a), beam quality at different output power (b) and a typical M^2 measurement at 6 W of output power (c) of the Ho:LuAG SCF laser.

A plano-convex spherical lens ($L3$, $f = 100 \text{ mm}$) and a CCD camera (WinCamDIR-BB, Dataray Inc.) was used to assess the beam quality of the Ho:LuAG SCF laser. A dichroic mirror (highly reflective to laser) and ND filter have been used to weaken the laser power during the measurement of M^2 , and the beam profile. As depicted in Figure 5(b), the beam quality at different output power was measured. As the output power increase from 1 W to 6 W, the values increased from 1.6 to 1.98 along x -axis, while from 1.78 to 2.04 along y -axis. Figure 5(c) shows a typical M^2 -factor measurement at an output power of 6 W, the inconsistency of values in the two directions may be caused by different heat dissipation effects in x - and y -directions, and the corresponding far-field beam profile are also shown in the insert of Figure 5(c). In this case, the measured M^2 -factor is larger than the value in Ho:YAG SCF (below 1.1) [12].

4. Conclusions

In conclusion, a 165-mm long, 0.5 at.% Ho:LuAG SCF with diameter less than 1 mm ($\sim 0.9 \text{ mm}$), has been grown by using the μ -PD method. From the spectral characterization, the absorption coefficient at 1907 nm was calculated to be 0.46 cm^{-1} , and the fluorescence spectrum is much similar to that of the Ho:LuAG bulk crystal. Limited by the feedback from the OCs to the high-brightness

fiber laser, a maximum output power of 1.86 W with a slope efficiency of 53% was achieved in free-space propagation pump configuration. For the pump guiding configuration with a laser diode, a maximum output power of 6.01 W with a slope efficiency of 42% was achieved, further power scaling is just limited by the available pump power. A higher slope efficiency of 52% was obtained with $T_{OC} = 50\%$, similar to that obtained with high-brightness pump, which indicates the pump guiding is also a good alternative for the Ho:LuAG SCF laser. The intrinsic loss of 0.021 cm^{-1} and minor fluctuation of the beam propagation factor with respect to the pump power also shows the good quality of the Ho:LuAG SCF, and have the prospect to be used in $2 \mu\text{m}$ spectral range.

Further power scaling of Ho:LuAG SCF by using high power 1908 nm laser diodes will be our priority. Due to the weaker nonlinear effects [34] and the larger thermal conductivity [12] compared to the conventional glass fiber, direct amplification (without chirped pulse stretching [34]) of ultrashort pulses by using such Ho-SCFs towards high-peak-power and high-energy in the $2 \mu\text{m}$ spectral range is also expected. On the other side, in comparison with the Tm:YAG SCF (propagation loss of 0.008 cm^{-1}) fabricated by mechanical method [35], the optical quality of the Ho:LuAG SCF are still need to be further improved, as well as decrease of the fiber diameter for better thermal mitigation.

Funding. National Natural Science Foundation of China (52032009, 61621001, 61975071, 62075090); Natural Science Foundation of Jiangsu Province (SBK2019030177).

Disclosures. The authors declare no conflicts of interest.

Data availability. Data underlying the results presented in this paper are not publicly available.

References

1. J. Ma, Z. P. Qin, G. Q. Xie, L. J. Qian, and D. Y. Tang, "Review of mid-infrared mode-locked laser sources in the $2.0 \mu\text{m}$ – $3.5 \mu\text{m}$ spectral region," *Appl. Phys. Rev.* **6**(2), 021317 (2019).
2. W. Kim, S. R. Bowman, C. Baker, G. Villalobos, B. Shaw, B. Sadowski, M. Hunt, I. Aggarwal, and J. Sanghera, "Holmium-doped laser materials for eye-safe solid state laser application," *Proc. SPIE* **9081**, 908105 (2014).
3. K. Scholle, E. Heumann, and G. Huber, "Single mode Tm and Ho:LuAG lasers for LIDAR applications," *Laser Phys. Lett.* **1**(6), 285–290 (2004).
4. G. J. Koch, B. W. Barnes, M. Petros, J. Y. Beyon, F. Amzajerdian, J. Yu, R. E. Davis, S. Ismail, S. Vay, M. J. Kavaya, and U. N. Singh, "Coherent differential absorption lidar measurements of CO_2 ," *Appl. Opt.* **43**(26), 5092–5099 (2004).
5. F. Gibert, D. Edouart, C. Cénac, and F. L. Mounier, "2- μm high-power multiple-frequency single-mode Q-switched Ho:YLF laser for DIAL application," *Appl. Phys. B* **116**(4), 967–976 (2014).
6. I. Mingareev, F. Weirauch, A. Olowinsky, L. Shah, P. Kadwani, and M. Richardson, "Welding of polymers using a $2 \mu\text{m}$ thulium fiber laser," *Opt. Laser Technol.* **44**(7), 2095–2099 (2012).
7. A. Dergachev, D. Armstrong, A. Smith, T. Drake, and M. Dubois, "3.4- μm ZGP RISTRA nanosecond optical parametric oscillator pumped by a 2.05- μm Ho:YLF MOPA system," *Opt. Express* **15**(22), 14404–14413 (2007).
8. S. A. Payne, L. L. Chase, L. K. Smith, W. L. Kway, and W. F. Krupke, "Infrared Cross-Section Measurements for Crystals Doped with Er^{3+} , Tm^{3+} , and Ho^{3+} ," *IEEE J. Quantum Electron.* **28**(11), 2619–2630 (1992).
9. Y. L. Tang, L. Xu, M. J. Wang, Y. Yang, X. D. Xu, and J. Q. Xu, "High-power gain-switched Ho:LuAG rod laser," *Laser Phys. Lett.* **8**(2), 120–124 (2011).
10. F. Wang, J. W. Tang, C. F. Shen, J. Wang, D. Y. Tang, and D. Y. Shen, "Ho³⁺:Y₂O₃ ceramic laser generated over 113 W of output power at 2117 nm," *Opt. Lett.* **44**(24), 5933–5936 (2019).
11. X. Délen, L. D. A. Aubourg, F. Lesparre, I. Martial, J. Didierjean, F. Balembois, and P. Georges, "Single crystal fiber for laser sources," *Proc. SPIE* **9342**, 934201 (2015).
12. Y. G. Zhao, L. Wang, W. D. Chen, J. L. Wang, Q. S. Song, X. D. Xu, Y. Liu, D. Y. Shen, J. Xu, X. Mateos, P. Loiko, Z. P. Wang, X. G. Xu, U. Griebner, and V. Petrov, "35 W continuous-wave Ho:YAG single-crystal fiber laser," *High Power Laser Sci. Eng.* **8**, e25 (2020).
13. K. Lebbou, D. Perrodin, V. I. Chani, A. Brenier, O. Tillement, O. Aloui, J. M. Fourmigué, J. Didierjean, F. Balembois, and P. Gorges, "Fiber single-crystal growth from the melt for optical applications," *J. Am. Ceram. Soc.* **89**(1), 75–80 (2006).
14. M. Matsukura, O. Nakamura, S. Watanabe, A. Miyamoto, Y. Furukawa, Y. Sato, T. Taira, T. Suzudo, and H. Mifune, "Core-clad-type composites of Nd:GdVO₄ single crystal grown by the double die EFG method," in *Advanced Solid-State Photonics* (Optical Society of America, Washington) (2007).
15. A. S. S. de Camargo, L. A. O. Nunes, D. R. Ardila, and J. P. Andreeta, "Excited-state absorption and 1064-nm end-pumped laser emission of Nd:YVO₄ single-crystal fiber grown by laser-heated pedestal growth," *Opt. Lett.* **29**(1), 59–61 (2004).

16. J. Didierjean, M. Castaing, F. Balembois, and P. Georges, "High-power laser with Nd:YAG single-crystal fiber grown by the micro-pulling-down technique," *Opt. Lett.* **31**(23), 3468–3470 (2006).
17. J. L. Wang, Q. S. Song, Y. W. Sun, Y. G. Zhao, W. Zhou, D. Z. Li, X. D. Xu, C. F. Shen, W. C. Yao, L. Wang, J. Xu, and D. Y. Shen, "High-performance Ho:YAG single-crystal fiber laser in-band pumped by a Tm-doped all-fiber laser," *Opt. Lett.* **44**(2), 455–458 (2019).
18. Y. Y. Xue, N. Li, Q. S. Song, X. D. Xu, X. T. Yang, T. Y. Da, D. H. Wang, Q. G. Wang, D. Z. Li, Z. S. Wang, and J. Xu, "Spectral properties and laser performance of Ho:CNGG crystals grown by the micro-pulling-down method," *Opt. Mater. Express* **9**(6), 2490–24966 (2019).
19. S. Veronesi, Y. Z. Zhang, M. Tonelli, and M. Schellhorn, "Efficient laser emission in Ho³⁺:LiLuF₄ grown by micro-pulling down method," *Opt. Express* **20**, 18723–18731 (2012).
20. P. G. Klemens, "Thermal resistance due to point defects at high temperatures," *Phys. Rev.* **119**, 507–509 (1960).
21. C. Y. Ma, J. F. Zhu, X. Nan, Z. Q. Hu, Z. C. Wen, J. Q. Long, X. Y. Yuan, and Y. G. Cao, "Demonstration and CW laser performances of composite YAG/Nd:LuAG/YAG transparent laser ceramic," *J. Alloy. Comp.* **727**, 912–918 (2017).
22. D. Sangla, N. Aubry, A. Nehari, A. Brenier, O. Tillement, K. Lebbou, F. Balembois, P. Georges, D. Perrodin, J. Didierjean, and J. M. Fourmigue, "Yb-doped Lu₃Al₅O₁₂ fibers single crystals grown under stationary stable state for laser application," *J. Cryst. Growth* **312**, 125–130 (2009).
23. V. Kononets, E. Auffray, C. Dujardin, S. Gridin, F. Moretti, G. Patton, K. Pauwels, O. Sidletskiy, X. Xu, and K. Lebbou, "Growth of long undoped and Ce-doped LuAG single crystal fibers for dual readout calorimetry," *J. Cryst. Growth* **435**, 31–36 (2016).
24. E. V. Charnaya, C. Tien, and T. Y. Her, "Effect of substitutional order on the relaxation of aluminum nuclei in Y_(3-x)Lu_xAl₅O₁₂ mixed garnets," *Phys. Solid State* **45**, 1672–1675 (2003).
25. E. D. Filer, C. A. Morrison, G. A. Turner, and N. P. Barnes, "Theoretical Branching Ratios for the ⁵I₇ → ⁵I₈ Levels of Ho³⁺ in the Garnets A₃B₂C₃O₁₂ (A = Y, La, Lu, Gd; B = Al, Lu, Sc, Ga; C = Al, Ga)," in *Advanced Solid-State Lasers*, Vol. 6 of OSA Proceedings Series (Optical Society of America, Washington, D.C. pp. 354–369 (1990).
26. B. M. Walsh, G. W. Grew, and N. P. Barnes, "Energy levels and intensity parameters of Ho³⁺ ions in Y₃Al₅O₁₂ and Lu₃Al₅O₁₂," *J. Physics and Chemistry of Solids* **67**, 1567–1582 (2006).
27. C. Y. Li, T. F. Xie, Z. Y. B. Q. Yao, H. M. Kou, Y. B. Pan, and J. Li, "Polycrystalline Ho: LuAG laser ceramics: fabrication, microstructure, and optical characterization," *J. Am. Ceram. Soc.* **100**(5), 2081–2087 (2017).
28. D. W. Hart, "Room-temperature lasing of end-pumped Ho:Lu₃Al₅O₁₂," *Opt. Lett.* **21**(10), 728–730 (1996).
29. X. D. Xu, K. Lebbou, F. Moretti, K. Pauwels, P. Lecoq, E. Auffray, and C. Dujardin, "Ce-doped LuAG single-crystal fibers grown from the melt for high-energy physics," *Acta. Materialia* **67**, 232–238 (2014).
30. Y. Zhao, W. Zhou, X. Xu, and D. Shen, "Spectroscopic properties and pulsed laser performance of thulium-doped (Lu, Y)₃Al₅O₁₂ mixed crystal," *Opt. Mater.* **62**, 701–705 (2016).
31. J. Liu, J. F. Dong, Y. Y. Wang, H. Q. Yuan, Q. S. Song, Y. Y. Xue, J. Xu, P. Liu, D. Z. Li, K. Lebbou, Z. X. Wang, Y. G. Zhao, X. D. Xu, and J. Xu, "Laser operation of Tm:LuAG single-crystal fiber grown by the micro-pulling down method," *Crystals* **11**, 898 (2021).
32. X. Délen, S. Piehler, J. Didierjean, N. Aubry, A. Voss, M. A. Ahmed, T. Graf, F. Balembois, and P. Georges, "250 W single-crystal fiber Yb:YAG laser," *Opt. Lett.* **37**(14), 2898–2900 (2012).
33. J. Morris, N. K. Stevenson, H. K. Bookey, A. K. Kar, C. T. A. Brown, J.-M. Hopkins, M. D. Dawson, and A. A. Lagatsky, "1.9 μm waveguide laser fabricated by ultrafast laser inscription in Tm:Lu₂O₃ ceramic," *Opt. Express* **25**(13), 14910–14917 (2017).
34. F. Lesparre, J. T. Gomes, X. Délen, I. Martial, J. Didierjean, W. Pallmann, B. Resan, F. Druon, F. Balembois, and P. Georges, "Yb:YAG single-crystal fiber amplifiers for picosecond lasers using the divided pulse amplification technique," *Opt. Lett.* **41**(7), 1628–1631 (2016).
35. J. Liu, J. F. Dong, Y. Y. Wang, J. Guo, Y. Y. Xue, J. Xu, Y. G. Zhao, X. D. Xu, H. H. Yu, Z. P. Wang, X. G. Xu, W. D. Chen, and V. Petrov, "Tm:YAG single-crystal fiber laser," *Opt. Lett.* **46**(18), 4454–4457 (2021).